Separation Science and Technology
Publication details, including instructions for authors and subscription information:
http://www.informaworld.com/smpp/title~content=t713708471

Mathematical Modeling of Facilitated Liquid Membrane Transport Systems Containing lonically Charged Species

J. P. Leiber[a]; R. D. Noble[a]; J. D. Way[a]; B. R. Bateman[a]
[a] NATIONAL BUREAU OF STANDARDS, CENTER FOR CHEMICAL ENGINEERING, BOULDER, COLORADO

To cite this Article Leiber, J. P. , Noble, R. D. , Way, J. D. and Bateman, B. R.(1985) 'Mathematical Modeling of Facilitated Liquid Membrane Transport Systems Containing lonically Charged Species', Separation Science and Technology, 20: 4, 231 — 256

To link to this Article: DOI: 10.1080/01496398508060678

URL: http://dx.doi.org/10.1080/01496398508060678

SEPARATION SCIENCE AND TECHNOLOGY, 20(4), pp. 231-256, 1985

Mathematical Modeling of Facilitated Liquid Membrane Transport Systems Containing Ionically Charged Species

J. P. LEIBER, R. D. NOBLE, J. D. WAY, and B. R. BATEMAN

NATIONAL BUREAU OF STANDARDS
CENTER FOR CHEMICAL ENGINEERING 773.1
BOULDER, COLORADO 80303

Abstract

A numerical model is presented which solves the transient nonlinear system of partial differential equations governing the facilitated transport of ionically charged species through a liquid membrane. The mathematical model is derived in dimensionless form and solved numerically. Facilitation factors and electrical potentials across the membrane are computed and compared to experimental results. This model is useful in predicting transient concentration, flux, and electrical potential gradients provided that the values of the required physical constants are known. It was noticed that transient facilitation factors are not affected by the transient electrical potential buildup, which indicates that both the pure diffusion and the faciltated transport of permeate are affected equally by the electrical effects of the ionically charged species.

INTRODUCTION

Developing liquid membrane transport systems consists of choosing a liquid which is selective for a particular species. In the absence of reactions, charged particles, and fluid movement, the permeate is transported by diffusion through the membrane. The permeate specie must meet a set of solubility and chemical equilibria criteria favoring only that substance. Purely diffusive transport is generally slow and unproductive except in a few special cases. The method of facilitated transport using chemical complexation has been used to improve the performance of liquid membranes beyond the level attainable by pure diffusion.

0149-6395/85/2004-0231$3.50/0

In facilitated transport the liquid membrane contains a carrier substance which reacts reversibly with the permeate to form a complex. The complex will in turn diffuse in addition to the permeate, thereby augmenting the flux of permeate through the membrane. Decomplexing of the carrier from the permeate occurs due to pressure and/or concentration gradients or by applying an agent which has a greater affinity for the permeate than the carrier. Typical facilitated transport liquid membranes are a mixture of two or more species, one of which is the carrier and the others solvents and nonparticipating species. It is common in gas separations that these carrier species are ions formed from the dissociation of a salt in solution.

Electrolytic liquid membranes can utilize one more transport mechanism, that of ion migration due to electrical forces. When charged particles are unevenly distributed, electric fields are present and movement of the charged particles induces current. The forces resulting from the presence of ions in the system will alter the mass transport and can either augment or retard the total permeate flux. In any case, additional effects can be externally induced by placing the system in an electric field. This is referred to as forced facilitation.

An early discussion of ionic transport mechanisms was given by Shean and Sollner (*1*) and induced the electric field effects in the transport equations. Further observations were noted by Ward (*2*) when facilitated transport was induced by an electric field. Bdzil et al. (*3*) measured the experimental quantities and presented a detailed mathematical description of the physical phenomena. The mathematical results reproduced those from the laboratory insofar as the electrical potential buildup was concerned. Later, Moore and Schecter (*4*) performed a similar study with different chemical species and reported favorable results. It was demonstrated repeatedly that the electrical potential rapidly varies with time due to the concentration changes of the ions.

De Koning, Stroeve, and Meldon (*5*) investigated these effects with carbon dioxide. Their mathematical treatment was much more involved than previous work, but reduced to equivalent expressions and produced satisfactory results.

A textbook addendum was presented by Krishna and Standart (*6*) which discussed in detail the effects of multicomponent mass transfer interactions. The primary emphasis was on diffusion only, with convective transport being the only other effect considered. Presumably, the value of the binary diffusivities can account for the significant interactions and any others can be neglected. A large portion of the addendum dealt with approximations, analytical solutions, and applications.

Goddard (*7*) presented a detailed vector-tensor analysis of the electric field equations associated with mass transport of ions. In addition to the overall transport, the effects of electrical boundary layers were also described and consideration of these boundary layers was put into perspective. With the assumption that layers of electrical charges at the boundaries are minimized by fluid velocities and well-chosen supporting structure material, these electrical boundary layer effects were ignored in this model.

Another electrical effect was investigated by Desai and Stroeve (*8*) using a monolayer of oleic acid sandwiched between water and mercury. They graphically showed how capacitance and current changed as the electrical potential across the monolayer was varied. It can be inferred that since current flow and ionic flux are proportional, and since a liquid monolayer is a good membrane approximation, the flux of ions across a membrane can be related by similar changes in the electrical potential. The structure of their oleic acid monolayer was also predicted using electrical measurements.

Popov and Timofeeva (*9*) investigated the effects of an alternating electric field on the facilitated transport mechanism. Their conclusion was that any alternating current will set up longitudinal waves which will augment mass transport by convection and by enhancement of permeation at the boundaries of the membrane by agitation. This method of "forced facilitation" could be implemented in direct current applications using pulsating fields.

Meldon, Stroeve, and Gregiore (*10*) researched the electrical potential differences in the carbon dioxide–hemoglobin system and indicated that the alkalinity of the electrolyte was directly related to the electrical potential drop across the membrane. They found that the transport of carbon dioxide is promoted by the electrostatic interactions in the highly alkaline systems and retarded in systems of lower alkalinities.

Ruckenstein and Sasidhar (*11*) made a study of the transient behavior of the nitric oxide–ferrous ion system used by Ward (*2*). Their data showed a transient peak in the electrical potential across the membrane. A maximum value is attained before steady-state is achieved. Their theory is that the maximum potential occurs at the time the permeate goes through a transition from "seeing" the membrane as semi-infinite to actual thickness. Data gathered from their paper comprise the basis for one evaluation of the model presented here.

Forced facilitation is discussed in some detail by Ivory (*12*) wherein he compares electrically enhanced transport to the same system without the induced field. He concluded that transport can be accelerated and promoted using an externally applied electric field. Ruckenstein and Sasidhar (*13*) then presented a different mathematical and numerical scheme for the system they used previously. This scheme incorporated a relaxation technique, and the solution was in agreement with their laboratory results.

The objective of this study is to incorporate the electric field effect terms into the model presented by Folkner and Noble (*14*). Evaluation of the model is accomplished using the data from Folkner and Noble (*14*) and Ruckenstein and Sasidhar (*11*). Comparison of model results to experimental data for NO separation using the Fe^{2+} as the carrier in formamide solvent is studied. Finally, various applications of the model are demonstrated.

PHYSICAL AND MATHEMATICAL DESCRIPTION

The physical configuration of a typical liquid-membrane transport system is shown in Fig. 1. The system is considered to be infinite in the y and z rectangular coordinates so that end effects are ignored. The permeate A enters the control volume at $x = 0$ and may react reversibly with the carrier B to form the complex AB.

$$A^{z_A} + B^{z_B} \underset{k_2}{\overset{k_1}{\rightleftarrows}} AB^{(z_A+z_B)} \tag{1}$$

Here, k_1 and k_2 represent the forward and reverse reaction rate constants respectively; z is the ionic charge of the species. The permeate and complex simultaneously move through the membrane by diffusion and ion migration to the other semipermeable boundary at $x = L$, where decomplexation can occur, returning the carrier to its original state. Note that reaction takes place throughout the membrane. For general systems containing many species, the complexation is

$$\nu_1[1]^{z_1} + \nu_2[2]^{z_2} + \sum_{i=4}^{n} \nu_i[i]^{z_i} \underset{k_2}{\overset{k_1}{\rightleftarrows}} \nu_3[3]^{z_3} + \sum_{i=4}^{n} \nu_i[i]^{z_i} \tag{2}$$

where $[i]$ represents the label associated with component i. Here, components 1, 2, and 3 are A, B, and AB, respectively. Components 4 through n are the other species present in the control volume which do not react with the permeate, but cannot be neglected if they carry an electrical charge. ν_i is the stoichiometric coefficient for the ith species.

The rate of production for the ith species then is

$$R_i = \nu_i(k_1 C_A C_B - k_2 C_{AB}) \tag{3}$$

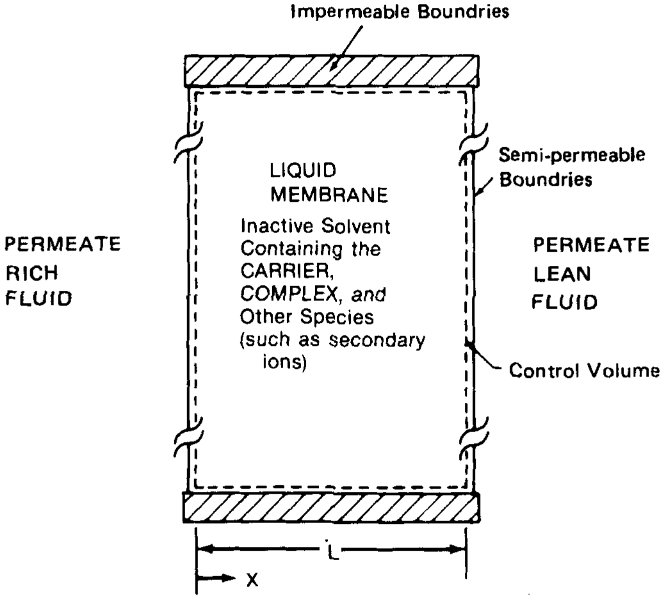

FIG. 1. Typical liquid membrane system.

where C_i is the concentration. The stoichiometric coefficients are determined directly from the reaction equation and compensate for the fact that moles are not conserved. To describe the molar flux relative to a stationary observer, the Nernst-Planck equation is used:

$$\mathbf{N}_i = \underset{\text{(flux due to convection)}}{vC_i} - \underset{\text{(flux due to diffusion)}}{D_i \nabla C_i} - \underset{\text{(flux due to electric field)}}{\frac{\beta}{RT} z_i D_i C_i \nabla \phi} \tag{4}$$

where v is the fluid velocity vector, D_i is the diffusivity of the ith species, β is Faraday's constant, R is the gas constant, T is the absolute temperature, and ϕ is the electrical potential. The continuity equation for each species i in the control volume is

$$\frac{\partial C_i}{\partial t} + \nabla \cdot \mathbf{N}_i = R_i \tag{5}$$

TABLE 1
Dimensionless Variables and Parameters

$C_i^* = \dfrac{C_i}{C_{A0}}$ = dimensionless concentration

C_{A0} = permeate concentration in liquid membrane which would be in equilibrium with permeate concentration in permeate-rich fluid

$D_i^* = \dfrac{D_i}{D_A}$ = dimensionless diffusivity

$\phi^* = \dfrac{\beta}{RT}\phi$ = dimensionless electrical potential

$\tau = \dfrac{D_A t}{L^2}$ = dimensionless time

$X = \dfrac{(x - x_1)}{L}$ = dimensionless position

$b = \dfrac{x_1}{L}$ = dimensionless radius of curvature

$\varepsilon = \dfrac{D_{AB}}{k_2 L^2}$ = inverse Damköhler number

$K = \dfrac{k_1}{k_2} C_{A0}$ = dimensionless reaction equilibrium constant

$\alpha = \dfrac{D_{AB}}{D_A} \dfrac{C_T}{C_{A0}}$ = mobility ratio (ratio of mobility of carrier to mobility of permeate)

C_T = initial carrier concentration

$\Delta = \dfrac{D_{AB}}{D_A} \dfrac{k_1}{k_2} C_T = \alpha K$

$\mathrm{Sh} = \dfrac{kL}{D_A}$ = Sherwood number for permeate mass transfer

k = mass transfer coefficient based on concentration driving force (see Eq. 21)

Assuming that D_i is constant and $v \to 0$ so that convection effects are neglected, substitution of Eqs. (3) and (4) into (5) yields

$$\frac{\partial C_i}{\partial t} = D_i \nabla^2 C_i + \frac{\beta}{RT} z_i D_i C_i \nabla^2 \phi + \nu_i (k_1 C_A C_B - k_2 C_{AB}) \qquad (6)$$

For the single-dimensional case, the Laplacian operator ∇^2 can be given by

$$\nabla^2 f = \frac{\partial^2 f}{\partial x^2} + \frac{a}{x} \frac{\partial f}{\partial x} \qquad (7)$$

where a is the geometry coefficient and x is the coordinate in the direction of mass transfer. (Note that x is the radial coordinate for cylindrical and spherical geometries.) For flat, cylindrical, and spherical geometries, a is 0, 1, and 2, respectively.

By redefining the variables in dimensionless form, as given in Table 1, Eq. (6), after some rearrangement, leads to

$$\frac{\partial C_i^*}{\partial \tau} = D_i^* \left\{ \frac{\partial^2 C_i^*}{\partial X^2} + \left(\frac{a}{X+b} \right) \frac{\partial C_i^*}{\partial X} + z_i C_i^* \left[\frac{\partial^2 \phi^*}{\partial X^2} + \left(\frac{a}{X+b} \right) \frac{\partial \phi^*}{\partial X} \right] \right\} + D_{AB}^* \nu_i \left(\frac{K}{\varepsilon} \right) \left[C_A^* C_B^* - \frac{1}{K} C_{AB}^* \right] \qquad (8)$$

which leads to the following equation for pure diffusion:

$$\frac{\partial C_i^*}{\partial \tau} = D_i^* \left\{ \frac{\partial^2 C_i^*}{\partial X^2} + \left(\frac{a}{X+b} \right) \frac{\partial C_i^*}{\partial X} \right\} \qquad (9)$$

The facilitation factor F is defined as the overall flux of the permeate at the effluxing boundary divided by the flux due only to diffusion:

$$F \equiv \left[\frac{\left(\dfrac{\partial C_A^*}{\partial X} \right)_{\text{total}}}{\left(\dfrac{\partial C_A^*}{\partial X} \right)_{\text{diffusion}}} \right] \Bigg|_{\text{at} X = 1} \qquad (10)$$

In order to expedite the calculation of the facilitation factor, it was necessary to introduce the dimensionless parameter Δ into Eq. (8) for the case where i is the permeate A.

$$\frac{\partial C_A^*}{\partial \tau} = \frac{\partial^2 C_A^*}{\partial X^2} + \left(\frac{a}{X+b}\right)\frac{\partial C_A^*}{\partial X} + z_A C_A^* \left(\frac{\partial^2 \phi^*}{\partial X^2} + \left(\frac{a}{X+b}\right)\frac{\partial \phi^*}{\partial X}\right] + \nu_A\left(\frac{\Delta}{\varepsilon C_T^*}\right)\left[C_A^* C_B^* - \frac{1}{K} C_{AB}^*\right] \tag{11}$$

where C_T is the total initial carrier concentration, defined as

$$C_T \equiv C_{AB} + C_B \tag{12a}$$

and

$$C_T^* = C_{AB}^* + C_B^* \tag{12b}$$

which lets the facilitation factor be computed as

$$F = \frac{\left(\dfrac{\partial C_A^*}{\partial X}\right)_{\Delta \neq 0,\, X=1}}{\left(\dfrac{\partial C_A^*}{\partial X}\right)_{\Delta = 0,\, X=1}} \tag{13}$$

There are several expressions one can use for ϕ^*, the local electrical potential. The two considered here are Poisson's equation [Chapman (*15*)] which is an alternate expression of Gauss' law

$$\nabla^2 \phi = -\frac{\beta}{\vartheta} \sum_{i=1}^{n} z_i C_i \tag{14}$$

where β is Faraday's constant, ϑ is a dielectric constant of the membrane, and the local electroneutrality assumption equation

$$\sum_{i=1}^{n} z_i C_i = 0 \tag{15}$$

which is valid for membranes thicker than 100 Å according to Ruckenstein

(*11*) and for electrical double layers and boundary layers of electrical charges according to Chapman (*15*).

Multiplying both sides of Eq. (8) by z_i and summing over all species leads to

$$\frac{\partial}{\partial \tau}\left(\sum_{i=1}^{n} z_i C_i^*\right) = \sum_{i=1}^{n}\left\{\frac{\partial^2 C_i^*}{\partial X^2} + \left(\frac{a}{X+b}\right)\frac{\partial C_i}{\partial X}\right\}$$

$$+ \sum_{i=1}^{n} z_i^2 C_i^* D_i^* \left\{\frac{\partial^2 \phi^*}{\partial X^2} + \left(\frac{a}{X+b}\right)\frac{\partial \phi^*}{\partial X}\right\} \qquad (16)$$

because $\Sigma\ z_i R_i = 0$ for species and charge continuity in the reaction. Applying Eq. (15) to Eq. (16) and rearranging gives

$$\frac{\partial}{\partial X}\left\{-\sum_{i=1}^{n} z_i^2 C_i^* D_i^* \left[\frac{\partial \phi^*}{\partial X} + \left(\frac{a}{X+b}\right)\phi^*\right]\right\}$$

$$= \frac{\partial}{\partial X}\left\{\sum_{i=1}^{n} z_i D_i^* \left[\frac{\partial C_i}{\partial X} + \left(\frac{a}{X+b}\right)\frac{\partial \phi^*}{\partial X}\right]\right\} \qquad (17a)$$

and when reduced by integration becomes

$$\frac{\partial \phi^*}{\partial X} + \left(\frac{a}{X+b}\right)\phi^* = -\frac{\sum_{i=1}^{n} z_i D_i^* \left[\frac{\partial C_i^*}{\partial X} + \left(\frac{a}{X+b}\right) C_i^*\right]}{\sum_{i=1}^{n} z_i^2 C_i^* D_i^*} \qquad (17b)$$

For flat geometries the equation is

$$\frac{\partial \phi^*}{\partial X} = -\frac{\sum_{i=1}^{n} z_i D_i^* \frac{\partial C_i^*}{\partial X}}{\sum_{i=1}^{n} z_i^2 C_i^* D_i^*} \qquad (17c)$$

When C_j^* is eliminated from Eq. (17c), the following relationship is obtained:

$$\frac{\partial \phi^*}{\partial X} = -\frac{\sum\limits_{\substack{i=1\\ i\neq j}}^{n} z_i(D_i^* - D_j^*)\dfrac{\partial C_i^*}{\partial X}}{\sum\limits_{\substack{i=1\\ i\neq j}}^{n} z_i C_i^*(z_i D_i^* - z_j D_j^*)} \tag{17d}$$

Since the right sides of Eqs. (17c) and (17d) are of the form (u/v), the Laplacian in Eq. (8) can be computed using the quotient rule of derivatives. Equations (17a)–(17d) can be modified for external electric fields if the forcing function is known.

Since each equation is first order in time and second order in space, each equation requires one initial condition and two boundary conditions.

Initial Condition

At $\tau = 0$: $C_1^* = C_A^* = 0$ (18a)

$C_2^* = C_B^* = C_T^*$ (18b)

$C_3^* = C_{AB}^* = 0$ (18c)

$C_i^* = C_{i0}^*$, for $i = 4, \ldots, n$ (18d)

Boundary Conditions

Case I — Concentration specified for A

At $X = 0$ $C_1^* = C_A^* = 1$ (19a)

$$\frac{\partial C_2^*}{\partial X} = \frac{\partial C_B^*}{\partial X} = 0 \tag{19b}$$

$$\frac{\partial C_3^*}{\partial X} = \frac{\partial C_{AB}^*}{\partial X} = 0 \tag{19c}$$

$$\frac{\partial C_i^*}{\partial X} = 0, \quad \text{for } i = 4, \ldots, n \tag{19d}$$

At $X = 1$ $C_1^* = C_A^* = 0$ (20a)

$$\frac{\partial C_2^*}{\partial X} = \frac{\partial C_B^*}{\partial X} = 0 \tag{20b}$$

$$\frac{\partial C_3}{\partial X} = \frac{\partial C^*_{AB}}{\partial X} = 0 \tag{20c}$$

$$\frac{\partial C_i}{\partial X} = 0, \qquad \text{for } i = 4, \ldots, n \tag{20d}$$

Since the liquid membrane is impermeable to all but species 1, the flux of species 2 through n will always be zero at the surface boundaries where $X = 0$ and $X = 1$.

Case II Flux specified for A

At $X = 0$
$$\frac{\partial C^*_1}{\partial X} = \frac{\partial C^*_A}{\partial X} = \text{Sh}(C^*_A - mC^*_{G,0}) \tag{21a}$$

$$\frac{\partial C^*_i}{\partial X} = 0, \qquad \text{for } i = 2, \ldots, n \tag{21b}$$

At $X = 1$
$$\frac{\partial C^*_1}{\partial X} = \frac{\partial C^*_A}{\partial X} = -\ \text{Sh}(C^*_A - mC^*_{G,1}) \tag{21c}$$

$$\frac{\partial C^*_i}{\partial X} = 0, \qquad \text{for } i = 2, \ldots, n \tag{21d}$$

where m is the ratio of gas solubility at current temperature and pressure to the ideal molar density of the bulk feed gas, and $C^*_{G,i}$ is the dimensionless concentration of the permeate in the bulk feed gas at $X = i$.

The solution procedure used PDECOL, a software package developed by Madson and Sincovec (*16*). The solution will take the form of arrays giving the value of each dependent variable, C^*_i, at each spatial point for every increment of time specified. Note that the dimensionless equations require no empirical (adjustable) parameters. The solution to the above equations was performed numerically to generate the C^*_i and the partial spatial derivatives of the C^*_i (i.e., the fluxes) as functions of time in discreet time steps.

The facilitation factor defined by Eq. (13) is useful in demonstrating the effectiveness of the carrier as a complexing agent versus the purely diffusive characteristics of the same system. If several carriers are available, the best choice could be easily determined by comparing facilitation factors. Another quantity of interest is the total electrical potential gradient across the membrane, defined as

$$\Delta V = \left.\frac{\partial \phi^*}{\partial X}\right|_{X=1} - \left.\frac{\partial \phi^*}{\partial X}\right|_{X=0} \tag{22}$$

By looking at this value, one can observe the charged particle effects on the mass transport and determine whether the effects are helpful or detrimental to the separation process. Actual values of compensating external fields can be suggested and added to the system to overcome any unwanted effects. By combining the resulting concentration and flux profiles, facilitation factors, and potential gradients, one can propose certain standards in scaling up laboratory prototypes to industrial applications.

MODEL EVALUATION

Model evaluations were made with the assumption that $D_{\mathrm{AB}} = D_{\mathrm{B}}$ and that there were negligible contributions from any species other than A, B, and AB. Noting that $z_{\mathrm{A}} = 0$ for an undissociated gas and substituting the values for species AB into those subscripted j, Eq. (17d) reduces to

$$\partial \phi^* / \partial X = 0 \tag{23}$$

Substitution of Eq. (23) into Eqs. (8) and (11) results in the following simplified equations:

$$\frac{\partial C_{\mathrm{A}}^*}{\partial \tau} = \frac{\partial^2 C_{\mathrm{A}}^*}{\partial X^2} + \left(\frac{a}{X+b}\right)\frac{\partial C_{\mathrm{A}}^*}{\partial X} + \nu_{\mathrm{A}}\left(\frac{\Delta}{\varepsilon C_T^*}\right)\left[C_{\mathrm{A}}^* C_{\mathrm{B}}^* - \frac{1}{K} C_{\mathrm{AB}}^*\right] \tag{24a}$$

$$\frac{\partial C_{\mathrm{B}}^*}{\partial \tau} = D_{\mathrm{B}}^*\left\{\frac{\partial^2 C_{\mathrm{B}}^*}{\partial X^2} + \left(\frac{a}{X+b}\right)\frac{\partial C_{\mathrm{B}}^*}{\partial X}\right\} + \nu_{\mathrm{B}} D_{\mathrm{AB}}^*\left(\frac{\kappa}{\varepsilon}\right)\left[C_{\mathrm{A}}^* C_{\mathrm{B}}^* - \frac{1}{\kappa} C_{\mathrm{AB}}^*\right] \tag{24b}$$

$$\frac{\partial C_{\mathrm{AB}}^*}{\partial \tau} = D_{\mathrm{AB}}^*\left\{\frac{\partial^2 C_{\mathrm{AB}}^*}{\partial X^2} + \left(\frac{a}{X+b}\right)\frac{\partial C_{\mathrm{AB}}^*}{\partial X}\right\} + \nu_{\mathrm{AB}} D_{\mathrm{AB}}^*\left(\frac{\kappa}{\varepsilon}\right)\left[C_{\mathrm{A}}^* C_{\mathrm{B}}^* - \frac{1}{\kappa} C_{\mathrm{AB}}^*\right] \tag{24c}$$

From Eq. (12b) one can see that

$$C_{\mathrm{B}}^{*} = C_{T}^{*} - C_{\mathrm{AB}}^{*} \tag{25}$$

Substitution of Eq. (25) into (24b) and into (24c) results in the same equation, since $D_{\mathrm{B}}^{*} = D_{\mathrm{AB}}^{*}$ and $\nu_{\mathrm{B}} = -1$ and $\nu_{\mathrm{AB}} = +1$. Thus, what was three equations now becomes the following two:

$$\frac{\partial C_{\mathrm{A}}^{*}}{\partial \tau} = \frac{\partial^{2} C_{\mathrm{A}}^{*}}{\partial X^{2}} + \left(\frac{a}{X+b}\right)\frac{\partial C_{\mathrm{A}}^{*}}{\partial X} + \nu_{\mathrm{A}}\left(\frac{\Delta}{\varepsilon C_{T}^{*}}\right)\left[C_{\mathrm{A}}^{*}(C_{\mathrm{T}}^{*} - C_{\mathrm{AB}}) - \frac{1}{\kappa}C_{\mathrm{AB}}^{*}\right] \tag{26a}$$

$$\frac{\partial C_{\mathrm{AB}}^{*}}{\partial \tau} = D_{\mathrm{AB}}^{*}\left\{\frac{\partial^{2} C_{\mathrm{AB}}^{*}}{\partial X^{2}} + \left(\frac{a}{X+b}\right)\frac{\partial C_{\mathrm{AB}}^{*}}{\partial X}\right\} + \nu_{\mathrm{B}} D_{\mathrm{AB}}^{*}\left(\frac{\kappa}{\varepsilon}\right)\left[C_{\mathrm{A}}^{*}(C_{\mathrm{T}}^{*} - C_{\mathrm{AB}}^{*}) - \frac{1}{\kappa}C_{\mathrm{AB}}^{*}\right] \tag{26b}$$

and the value of ΔV reduces to

$$\Delta V = \frac{RT}{q\beta}\ln\left(\frac{C_{\mathrm{A}}^{*}|_{X=1}}{C_{\mathrm{A}}^{*}|_{X=0}}\right) \tag{27}$$

where q is the number of electrons liberated between membrane species.

After Eqs. (26) and (27) were incorporated into the computer programs, testing commenced with values of κ, ε, and Δ presented by Folkner and Noble (*14*) for uncharged systems. The values were compared and complete agreement was observed as shown in Fig. 2.

A second test was made using the data provided by Ruckenstein and Sasidhar (*11*). A transient plot of ΔV reproduced their results exactly and is shown in Fig. 3.

MODEL APPLICATION

Upon successful completion of the model testing, experimental data were analyzed [Bateman and Way (*17*)]. The values of k_1 and k_2, the forward and reverse reaction rate constants, were unknown. The value of D_{AB} was

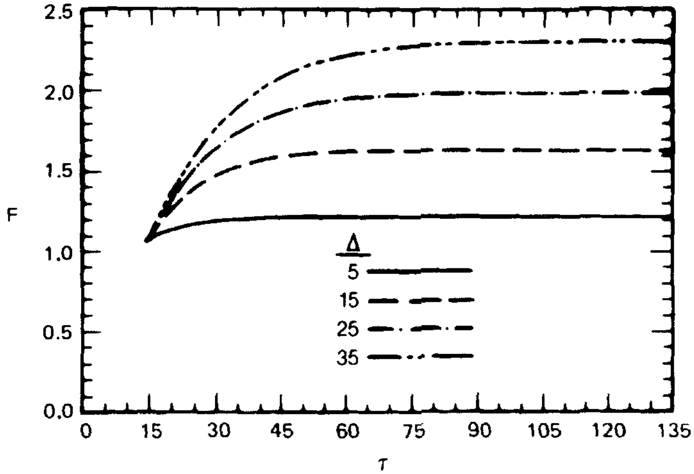

Transient Facilitation Factors vs Dimensionless Time using data from Folkner and Noble (1983). Input values of Delta are given in the legend. Other Input values are:
a=0, b=.1, T=25°C, q=1, $D_A^* = 1.0$, $D_{AB}^* = D_B^* = 0.1$, $z_A = z_B = z_{AB} = 0$, $C_{A0}^* = 1$, $C_{B0} = C_T^* = 1$, $\nu_A = -1$, $\nu_B = +1$, $\varkappa = 1.0$, $\varepsilon = 1.0$

FIG. 2. Evaluation of model using neutral species.

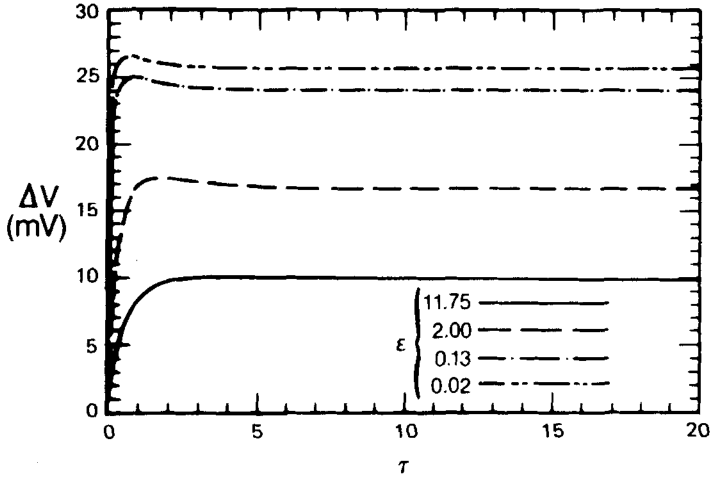

Electrical Potential Drop vs Dimensionless Time using data given in Ruckenstein and Sasidhar (1982). Input values of Epsilon are given in the legend. The other input values are:
a=0, b=0.1, T=23°C, q=1, $D_A^* = 1.0$, $D_{AB}^* = D_B^* = 0.13245$, $z_A = 0$,
$z_B = z_{AB} = +2$, $C_{AB}^* = 1$, $C_{B0}^* = C_T^* = 95.42$, $\nu_A = -1$, $\nu_B = +1$, $\varkappa = 2.08028$,
$\Delta = 26.291325$

FIG. 3. Evaluation of model using ionically charged species.

TABLE 2
Laboratory Data and Experimentally Determined Physical Properties [17]

$T = 25°\text{C}$
$P = 84.0\ \text{kPa}$
A = NO
B = Fe^{2+}
AB = $FeNO^{2+}$
Solvent = $HCONH_2$
$C_T = 3.0 \times 10^{-4}\ \text{mol/cm}^3$
$D_A = 3.16 \times 10^{-5}\ \text{cm}^2/\text{s}$
$S = 2.5 \times 10^{-6}\ \text{mol/cm}^3$
$L = 0.0304\ \text{cm}$

The following were estimated:

$D_{AB} = 1.23 \times 10^{-5}\ \text{cm}^2/\text{s}$
$K_{eq} = 1.1 \times 10^5\ \text{cm}^3/\text{mol}$
$k_2 = 1.4 \times 10^2\ \text{s}^{-1}$
$\Psi = 0.615$ = porosity

Y_{A0}	$F_{\text{steady-state}}$
0.2	5.5
0.4	3.8
0.6	3.0
0.8	2.5
1.0	2.2

assumed to be equal to D_B, which was reported as 1.23×10^{-5} cm²/s, an order of magnitude different from the value indicated by Ward (*2*) of 2.0×10^{-6} cm²/s. The first application of this model did not reproduce the results found in the laboratory. Using $k_2 = 9.0 \times 10^{-3}\ \text{s}^{-1}$, $K_{eq} = 1.1 \times 10^5$ cm³/mol, and the values shown in Table 2, this model gave F (with $Y_{A0} = 0.2$) = 1.72 and F (with $Y_{A0} = 1.0$) = 1.65. Y_{A0} is the mole fraction of permeate in the feed. With the uncertainty of the above parameters, it was decided to search for the combination of values which gave results similar to those determined experimentally.

The search procedure began by holding the value of Δ constant and selecting the other parameters at random. The selection of K_{eq} determined the values of K corresponding to the initial bulk concentration of the permeate in the feed gas, as given by

$$K = Y_{A0} K_{eq} S \tag{28}$$

TABLE 3
Model Parameters Used in First Search with $\Delta = 25$

K_{eq} (cm^3/mol)	D^*_{AB} (dimensionless)	κ (dimensionless)				
		$Y_{A0} = 0.2$	$Y_{A0} = 0.4$	$Y_{A0} = 0.6$	$Y_{A0} = 0.8$	$Y_{A0} = 1.0$
8.32×10^5	0.1	0.416	0.832	1.248	1.664	2.08
2.08×10^6	0.04	1.04	2.08	3.12	4.16	5.2
2.5×10^6	0.0333	1.25	2.5	3.75	5.0	6.25
3.0×10^6	0.0278	1.5	3.0	4.5	6.0	7.5
4.0×10^6	0.02083	2	4	6	8	10

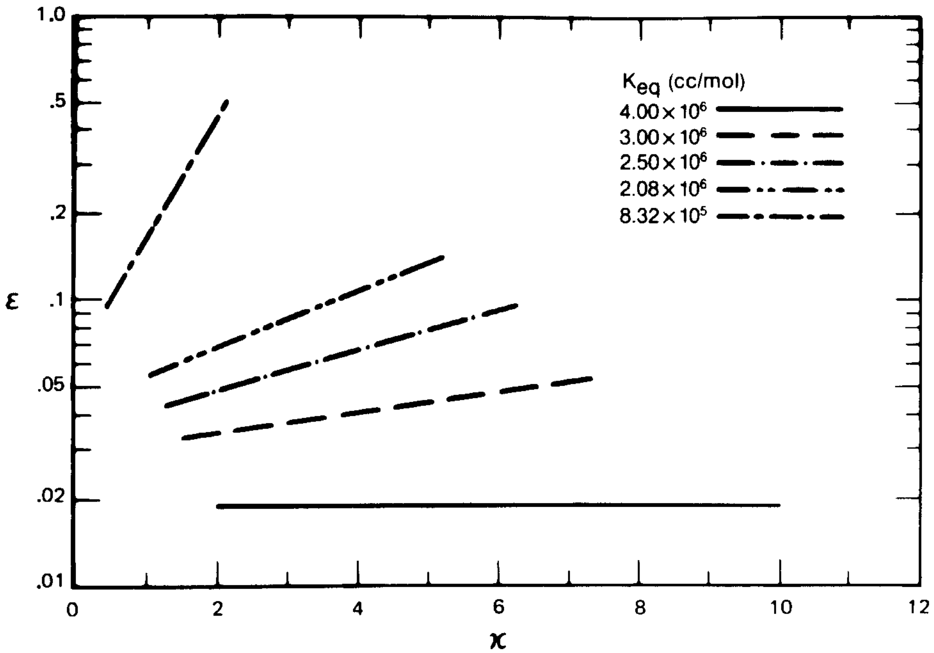

FIG. 4. Parameter search for $\Delta = 25$.

where K_{eq} is the reaction equilibrium constant in cm^3/mol, and S is the solubility of the permeate in the liquid membrane solution at the existing temperature and pressure.

Table 3 shows the values of the model parameters used in the first search. D^*_{AB} was determined from the definition of Δ in Table 1 and given by

$$D^*_{AB} = \frac{\Delta}{K_{eq}C_T} \tag{29}$$

Subsequently, values of the ε's which gave the same value for the experimental steady-state facilitation factors were plotted versus the value of K corresponding to the experimental mole fraction of the permeate as shown in Fig. 4. It was observed that as K_{eq} increased, the variation in the values of ε decreased. The goal was to have ε remain constant for all five values of K plotted at that particular K_{eq}. For $\Delta = 25$ this occurred at $K_{eq} = 4.0 \times 10^6$ cm^3/mol and resulted in $\varepsilon = 0.0186$ when the experimental model facilitation factors were the same. The values of D_{AB}, k_1, and k_2 were computed using Eq. (29) and

$$D_{AB} = D^*_{AB} D_A \tag{30}$$

$$k_2 = \frac{D_{AB}}{\varepsilon L^2} \tag{31}$$

$$k_1 = \frac{k_2 \Delta}{D^*_{AB} C_T} \tag{32}$$

The resulting $D_{AB} = 6.58 \times 10^{-7}$, which is an order of magnitude smaller than Ward's (*2*) value.

Next, values of Δ were varied, and the sets of parameters that gave the correct solution were found for each Δ. Table 4 shows the complete results of this search procedure. Figures 5 and 6 graphically show the infinite sets of parameters Δ, ε, and K_{eq} which will reproduce the experimental results. Of special interest is the data set at $\Delta = 100$, $K_{eq} = 7.2 \times 10^6$ cm³/mol, and $\varepsilon = 0.16$. With this combination, $D_{AB} = 1.46 \times 10^{-6}$ cm²/s, which is closest to the value reported by Ward (*2*). The values of k_2 and k_1 are also very close to those found in the literature. Therefore, this is the best steady-state data set available for the concentration specified boundary conditions (Case I).

The next step was to match transient data with an optimum set of parameters. Experimental transient data were available only for the case of $Y_{AO} = 1.0$ and are given in Table 5. The transient data produced by the model were plotted with the experimental data and are shown in Fig. 7. Calculating the standard deviation of the experimental values from the

TABLE 4

Data Sets Satisfying Experimental Results Using the Concentration Specified Boundary Conditions

Δ	ε	κ	K_{eq}	D_{AB}	k_1	k_2
at $Y_{AO} = 1.0$			(cm³/mol)	(cm²/s)	(cm³/mol · s)	(s⁻¹)
25	0.0186	10.0	4.0×10^6	6.58×10^{-7}	1.53×10^5	3.83×10^{-2}
30	0.03	10.5	4.2×10^6	7.51×10^{-7}	1.13×10^5	2.71×10^{-2}
45	0.07	11.5	4.6×10^6	1.03×10^{-6}	7.33×10^4	1.59×10^{-2}
100	0.16	18.0	7.2×10^6	1.46×10^{-6}	7.36×10^4	9.87×10^{-3}
300	0.53	25.0	1.0×10^7	3.16×10^{-6}	6.45×10^4	6.45×10^{-3}

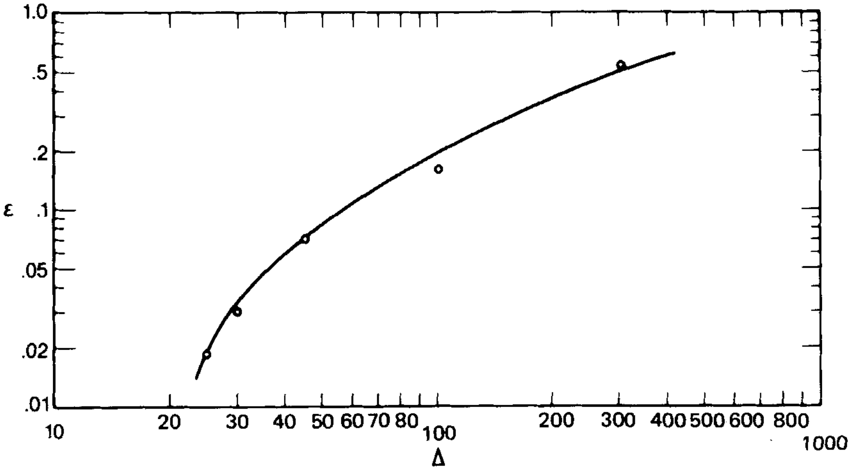

FIG. 5. ε vs Δ for Case I boundary conditions.

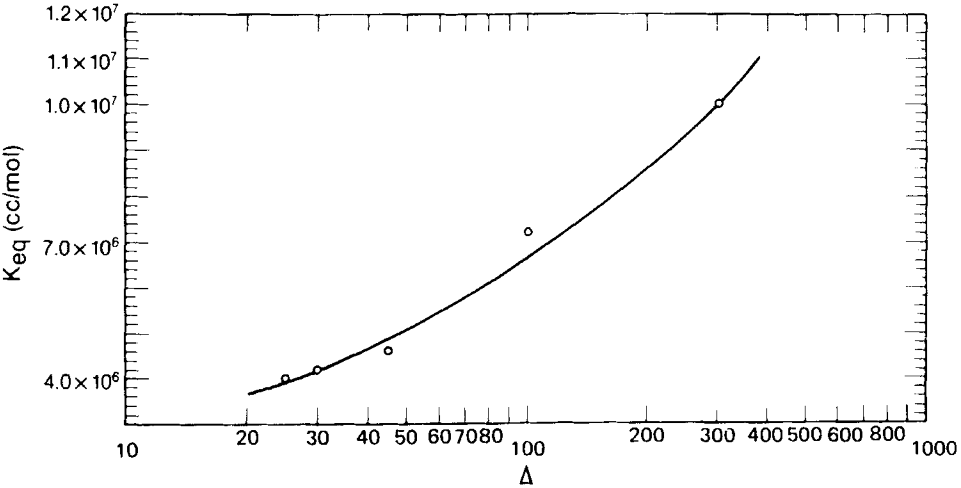

FIG. 6. K_{eq} vs Δ for Case I boundary conditions.

TABLE 5
Experimental Transient Data (*17*) at $Y_{A0} = 1.0$ for NO–Fe^{2+} System
N_A (diffusion) = 2.6×10^{-9} mol/cm$^2 \cdot$ s

t (min)	τ (dimensionless)	N_A (mol/cm$^2 \cdot$ s)	F (dimensionless)
3.34	6.86	2.1×10^{-9}	0.808
5.34	10.96	3.75×10^{-9}	1.442
7.34	15.07	4.46×10^{-9}	1.715
9.34	19.07	4.88×10^{-9}	1.877
11.34	23.28	5.11×10^{-9}	1.965
13.34	27.38	5.30×10^{-9}	2.038
15.34	31.45	5.41×10^{-9}	2.081
17.34	35.55	—	—
19.34	39.70	5.64×10^{-9}	2.170
∞	∞	5.72×10^{-9}	2.200

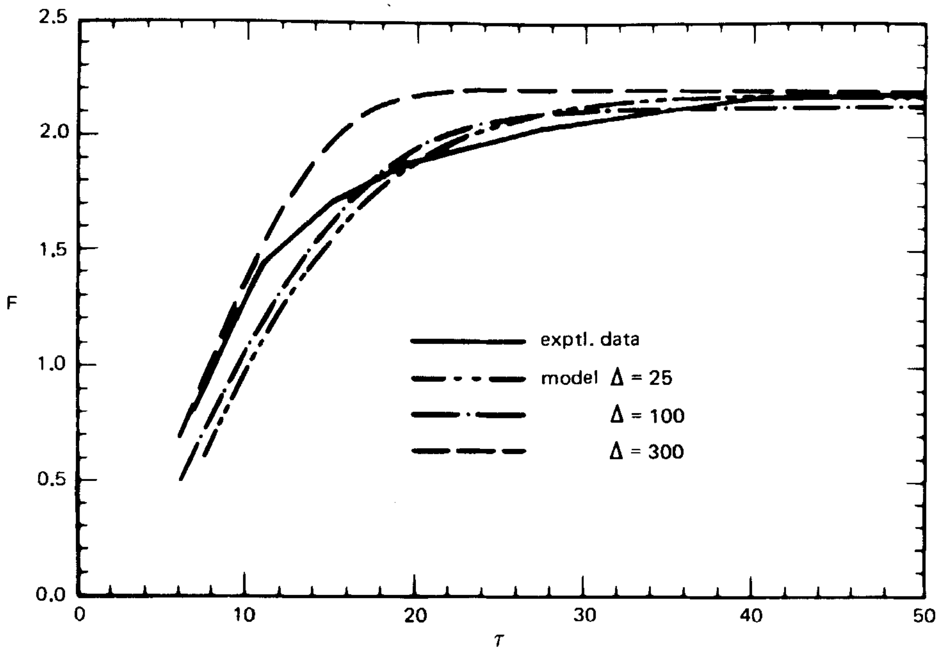

FIG. 7. Transient facilitation factors (model compared to experimental data for Case I boundary conditions).

TABLE 6
Search Technique for $\Delta = 300$ Using Flux Boundary Conditions (Case II)

Sh	K_{eq} (cm^3/mol)	ε, where $F(Y_{A0} = 1.0) = 2.2$	Corresponding $F(Y_{A0} = 0.2)$
10	1.0×10^7	0.02	4.5
20	1.0×10^7	0.2	4.9
20	1.4×10^7	0.015	6.0
20	1.6×10^7	0.0001	6.2
30	1.2×10^7	0.2	5.8
30	1.4×10^7	0.05	6.2
40	1.4×10^7	0.08	6.3

model-generated numbers resulted in choosing $\Delta = 100$ as the best fit. Therefore, the best values of the unknown constants are:

$$D^*_{AB} = 0.0462, \qquad D_{AB} = 1.46 \times 10^{-6} \text{ cm}^2/\text{s}$$

$$k_1 = 7.36 \times 10^4 \text{ cm}^3/\text{mol} \cdot \text{s}, \qquad k_2 = 9.87 \times 10^{-3} \text{ s}^{-1}$$

and

$$K_{eq} = 7.2 \times 10^6 \text{ cm}^3/\text{mol}$$

Both steady-state and transient procedures were repeated for the flux specified boundary conditions (Case II). The method used to search for the theoretical data sets was different than the one used for Case I. Since the Sherwood number is another parameter to vary, the search procedure was modified by first choosing a value for Δ. Various values of Sh were chosen, and the K_{eq}–ε combinations that gave the desired facilitation factors were sought. A graph of the resulting facilitation factor at $Y_{AO} = 0.2$ was plotted versus K_{eq} for each run at the value of ε and Sh which gave the facilitation factor of 2.2 at $Y_{AO} = 1.0$. For $\Delta = 300$, Table 6 shows the values generated by the model and graphed on Fig. 8. The line across the center at $F = 5.5$ represents the infinite number of solution sets. Lines of constant Sh and constant ε were approximated using the data points available.

The solution set at $K_{eq} = 1.2 \times 10^7$ cm^3/mol was estimated using Fig. 8. The estimated values of Sh = 22 and $\varepsilon = 0.1$ were close, and one more run refined the set to $\varepsilon = 0.075$.

For a $\Delta = 25$, the search procedure was to be repeated. The two data sets

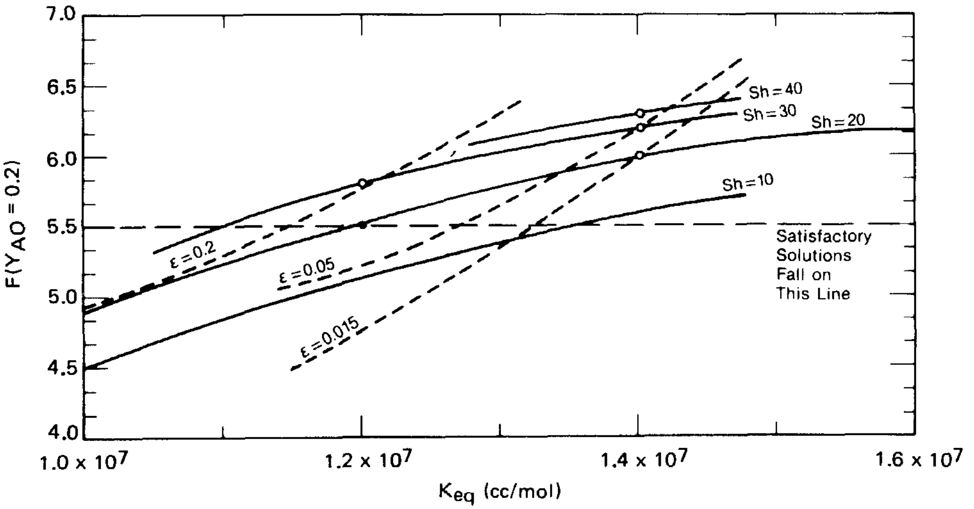

FIG. 8. Search technique for flux boundary conditions (Case II) = 300.

obtained occurred at Sh = 40, $K_{eq} = 4.0 \times 10^6$ cm^3/mol and $\varepsilon = 0.0015$, and at Sh = 50, $K_{eq} = 4.0 \times 10^6$ cm^3/mol and $\varepsilon = 0.003$.

Since the experimental transient data are scarce, the three solution sets shown in Table 7 were plotted with the transient laboratory results and a selection of the best fit was made from that. Figure 9 shows this transient match up. It appears that the Sherwood number has a very small effect at lower values of Δ. The most significant effect is on the reaction equilibrium data; as the Sherwood number increases, K_{eq} decreases, and the boundary conditions approach those in Case I.

It should be pointed out that Ward (2) estimated the value of D_{AB} at 2×10^{-6} cm^2/s. Since the best values of D_{AB} determined by using this model gave values close to this one, it is assumed that the choice was reasonable. The values of k_1, k_2, and K_{eq} found in the literature range over several orders of magnitude and suggest that these values are not well established.

The usefulness of the permeate flux boundary condition can be shown by applying the sum of the resistances technique. For the flux condition (Case II) the total resistance to mass transport is given by

$$R = \frac{2}{k} + \frac{L}{FD_A} \tag{33}$$

TABLE 7

Data Sets Satisfying Experimental Results Using Flux Boundary Conditions (Case II)

Δ	Sh	ε	$K_{(Y_{A0}=1.0)}$	K_{eq} (cm^3/mol)	D_{AB} (cm^2/s)	k_1 (cm^3/mol · s)	k_2 (s^{-1})
300	22	0.075	30	1.2×10^7	2.63×10^{-6}	4.56×10^5	3.80×10^{-2}
25	40	0.0015	10	4.0×10^6	6.58×10^{-7}	1.90×10^6	4.75×10^{-2}
25	50	0.003	10	4.0×10^6	6.58×10^{-7}	9.50×10^5	2.37×10^{-1}

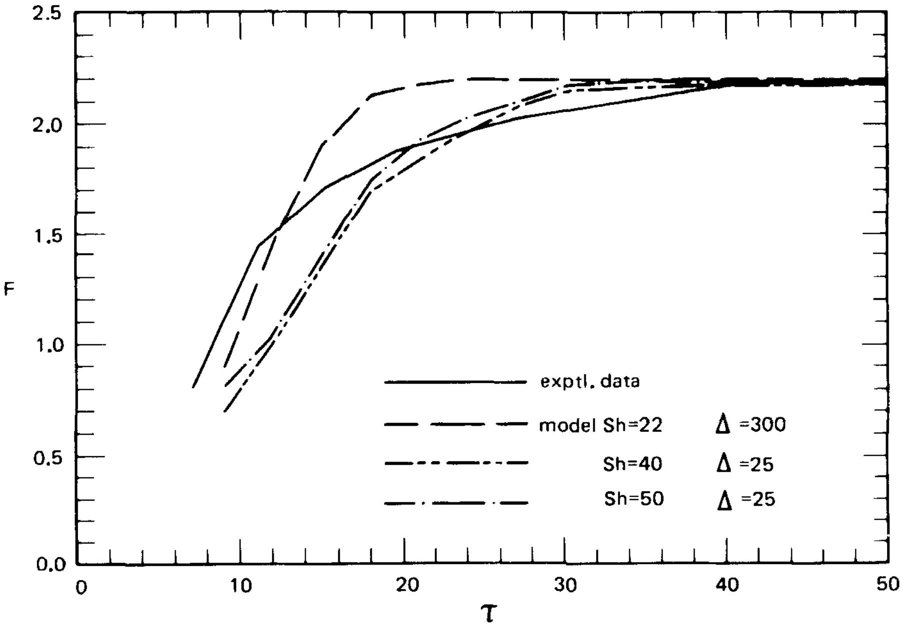

FIG. 9. Transient facilitation factors (model compared to experimental data for Case II boundary conditions).

where the first term represents the combined resistances through the interfacial boundary layers on both sides of the membrane, and the second term is the total resistance across the membrane itself. For high initial concentrations of permeate in the bulk feed, the contribution of the first term is less than one-quarter of the total resistance (17% for $Y_{AO} = 1.0$). For low initial concentrations the contribution is as much as one-third of the total. Therefore, neglecting this boundary layer will have an effect on the solution.

DISCUSSION

The mathematical model presented here, which includes electric field effects, produces favorable solutions to the one-dimensional set of partial differential equations governing a typical liquid membrane system. Evaluation of the model was accomplished and its validity was confirmed. The use of the flux boundary condition (Case II) is more exact, but requires more computing time.

Regardless of which boundary condition was implemented, it was found that the facilitation factors vary more with changes in initial permeate concentration as the reaction equilibrium constant decreases. Therefore, the faster the forward reaction of the permeate is with the carrier, the higher the facilitation factor. The variation of Δ and K_{eq} that gives the same solution is nearly linear with respect to the logarithm of Δ. Also, the logarithmic changes that affect Δ cause the logarithm of ε to change in a nearly linear fashion to produce the same solution. The mere fact that many combinations of the variables D_{AB}, k_1, and k_2 will give the same solution places emphasis on determining these constants experimentally.

For the flux boundary condition (Case II), it was found that increases in the Sherwood number will increase facilitation, which can be justified by noting that as Sh approaches infinity, the flux boundary condition becomes the concentration boundary condition. As Sh increases, the ε required to get the same solution also increases; however, ε does not increase linearly with Sh. There seems to be a limiting value of Sh near 10 where the value of ε becomes nearly zero and the solution procedure no longer is valid. This can be explained by assuming that at this limit the resistance to mass transfer becomes infinite.

This model can be expanded. The assumption that $D_{AB} = D_B$ can be omitted. If neither is known, each can be sought, or if one is known, the other can be found. Variations in membrane thickness and membrane shape can also be researched using this model. Ionically dissociated liquids can be studied without neglecting the electrical potentials developed. The mathematical model can also be combined with other models to give electrical effects. For instance, competitive transport [Niiya (*18*)] and two-dimensional flows, as in cylindrical continuous flow systems, are two possibilities for further study.

REFERENCES

1. G. M. Shean and K. Sollner, "Carrier Mechanisms in the Movement of Ions across Porous and Liquid Ion Exchange Membranes," *Ann. N. Y. Acad. Sci.*, *759* (1966).

2. W. J. Ward III, "Electrically Induced Carrier Transport," *Nature, 227* (July 11, 1970).

3. J. Bdzil, C. C. Carlier, H. L. Frisch, W. J. Ward III, and M. W. Breiter, "Analysis of Potential Difference in Electrically Induced Carrier Transport Systems," *J. Phys. Chem.*, *77*(6), 846 (1973).

4. J. H. Moore and R. S. Schechter, "Liquid Ion Exchange Membranes," *AIChE. J.*, *19*(4), 741 (July 1973).

5. J. de Koning, P. Stroeve, and J. H. Meldon, "Electrical Potentials during Carbon Dioxide Transport in Hemoglobin Solutions," *Adv. Exp. Med. Biol.*, *94*, 183 (1978).

6. R. Krishna and G. L. Standart, "Mass and Energy Transfer in Multicomponent Systems," *Chem. Eng. Commun.*, *3*, 201 (1979).

7. J. D. Goddard, "Electrical Field Effects in Carrier-Mediated Ion Transport," *AIChE Symp. Ser.: Transport with Chemical Reactions, 77*, 202 (1981).
8. N. Desai and P. Stroeve, "Application of an Electrode's Technique to Study Transport across Monolayers," *Chem. Eng. Commun., 11*, 113 (1981).
9. A. N. Popov and S. K. Timofeeva, "Effect of an Alternating Electric Field on the Transfer of Dicyanourate Ions across a Liquid Ion-Exchange Membrane by Direct Current," *Latv. PSR Zinat. Akad Vestis, Kim. Ser., 1*, 100 (1982) (in Russian).
10. J. H. Meldon, P. Stroeve, and C. E. Gregiore, "Facilitated Transport of Carbon Dioxide: A Review," *Chem. Eng. Commun., 16*, 263 (1982).
11. E. Ruckenstein and V. Sasidhar, "Transient Behavior of Facilitated Transport through Liquid Membranes," *J. Membr. Sci., 12*, 27 (1982).
12. C. F. Ivory, *Forced Facilitation in Carrier-Mediated Transport*, AIChE Paper No. 51f, November 16, 1982.
13. E. Ruckenstein and V. Sasidhar, "Relaxation Method for Facilitated Transport," *J. Membr. Sci., 13*, 67 (1983).
14. C. A. Folkner and R. D. Noble, "Transient Response of Facilitated Transport Membranes," *Ibid., 12*, 289 (1983).
15. T. W. Chapman, "Ionic Transport and Electrochemical Systems," *AIChE Continuing Educ. Ser. 4: Lect. Transp. Phenom.*, p. 90 (1969).
16. N. K. Madson and R. F. Sincovec, "PDECOL, General Collocation Software for Partial Differential Equations," *ACM Trans. Math. Software, 5*, 326 (1979).
17. B. R. Bateman and J. D. Way, *Facilitated Transport of Nitric Oxide*, Presented at the AIChE National Meeting, Denver, Colorado, August 1983.
18. K. Niiya and R. D. Noble, "Competitive Facilitated Transport through Liquid Membranes," *J. Membr. Sci., 23*, 183 (1985).

Received by editor December 26, 1984